# NS3 helicase actively separates RNA strands and senses sequence barriers ahead of the opening fork

Wei Cheng[†], Sophie Dumont[‡§], Ignacio Tinoco, Jr.[¶], and Carlos Bustamante[†¶‖††‡‡§§]

[†]QB3 Institute, [‡]Biophysics Graduate Group, Departments of [¶]Chemistry and [‖]Physics, and [††]Howard Hughes Medical Institute, University of California, Berkeley, CA 94720; and [‡‡]Physical Biosciences Division, Lawrence Berkeley National Laboratory, Berkeley, CA 94720

Edited by Stephen C. Kowalczykowski, University of California, Davis, CA, and accepted by the Editorial Board July 6, 2007 (received for review March 13, 2007)

**RNA helicases regulate virtually all RNA-dependent cellular processes. Although much is known about helicase structures, very little is known about how they deal with barriers in RNA and the factors that affect their processivity. The hepatitis C virus encodes NS3, an RNA helicase that is essential for viral RNA replication. We have used optical tweezers to determine at the single-molecule level how the local stability of the RNA substrate affects the enzyme rate of strand separation, whether separation occurs by an active or a passive mechanism, and whether processivity is affected. We show that sequence barriers in RNA modulate NS3 activity. NS3 processivity depends on barriers ahead of the opening fork. Our results rule out a model where NS3 passively waits for the thermal fraying of double-stranded RNA. Instead, we find that NS3 destabilizes the duplex before separating the strands. Failure to do so before a strong barrier leads to helicase dissociation and limits the processivity of the enzyme.**

hairpin | molecular motors | optical tweezers | processivity

A wide range of RNA metabolic activities (1) require the breaking of base pairs in double-stranded RNA (dsRNA) by RNA helicases. Despite recent progress in the study of these motor proteins (2–4), the physical mechanisms by which they move and catalyze the strand separation are not well understood. Helicase models ranging from a pure Brownian ratchet to a pure power stroke action have been discussed (5–8), but experimental data to support them for RNA helicases have been lacking. The hepatitis C virus NS3 protein is a superfamily 2, 3′ to 5′ RNA helicase (9) known to be essential for virus replication and, thus, an antiviral drug target (10). Recently, NS3 has been the subject of single-molecule manipulation studies (4), which revealed that NS3 makes steps of 11 bp each made up of three substeps (4). RNA molecules contain various kinetic barriers to mechanical unfolding (11). How these barriers influence the activity of motor proteins that work on RNA will depend on the mechanism of the motor. To probe the molecular mechanism of NS3 unwinding activity, we have designed and characterized RNA molecules with various mechanical unfolding barriers and used single-molecule methods to investigate how these barriers affect the velocity, pausing, and processivity of the helicase in real time.

## Results

**Design and Characterization of RNA Hairpin Substrates.** We first designed two RNA hairpin substrates that terminate both on a tetraloop (Fig. 1*A*) to monitor the response of a single NS3 helicase to weak and strong sequence barriers. Substrate RNA-AG has 30 A·U pairs followed by 30 G·C pairs; RNA-GA has the A·U and G·C sequences interchanged. The sequences within A·U and G·C regions were chosen to minimize the formation of alternative secondary structures other than the desired 60-bp hairpin. In our experiment, a single RNA hairpin was attached between a microsphere in an optical trap and a microsphere placed on the end of a micropipette through hybrid RNA–DNA handles to separate the hairpin from the surfaces (see Fig. 1*B* and *Materials and Methods*). Both substrates contain a 3′ single-stranded RNA (ssRNA) "launch pad" 10 nucleotides long (Fig. 1*B*) that facilitates NS3 loading. We first characterized the unfolding properties of these substrates by applying tension between the ends of each substrate using counterpropagating dual-beam, force-measuring optical tweezers (12, 13). As the tension cycled between 2 and 30 pN, we monitored the change in the end-to-end distance (i.e., extension) of the molecule. As shown in Fig. 1*C*, RNA-AG unfolds mechanically in two transitions: the first occurs at 11.3 ± 0.1 pN and corresponds to the unfolding of 30 A·U pairs; the second corresponds to the unfolding of the 30 G·C pairs and occurs at 26.2 ± 0.2 pN. In contrast, RNA-GA unfolds by mechanical force in a single transition at 26.0 ± 0.2 pN (Fig. 1*D*) and does not refold upon relaxation until the tension on the molecule drops below 11 pN (14). These results show that the mechanical stabilities of A·U and G·C pairs are distinct and that stretches of G·C pairs constitute barriers to RNA unfolding in these pulling experiments.

**Barrier Dependence of NS3 Pausing and Stepping.** To follow the unwinding of these substrates by NS3, we flowed NS3 and ATP together in buffer U into the fluidic chamber at 22 ± 1°C (5 nM NS3 and 1 mM ATP unless otherwise noted). We have shown previously that the helicase activity we monitored using this assay most likely originates from NS3 monomer (4). Independent from single-molecule experiments, we also did single-cycle unwinding experiments in bulk and showed that the NS3 monomer does have helicase activity, and its processivity is consistent with single-molecule observations [supporting information (SI) Fig. 7]. Next, using the constant force feedback mode of the instrument, RNA-AG was held at 7.0 ± 0.1 pN, while changes in its end-to-end distance were simultaneously monitored (4). At this force, no spontaneous opening of RNA-AG was observed in the absence of either NS3 or ATP. Therefore, the extension change of RNA-AG seen when both NS3 and ATP are present must be due to helicase-catalyzed hairpin unwinding and can be converted into the number of RNA base pairs unwound at the given force as a function of time (4, 15, 16).

Strikingly, NS3 unwinding is affected by the same sequence-dependent barriers in the RNA-AG hairpin seen in force unfolding (Fig. 2*A*). For most unwinding events (>80%), NS3 proceeds very rapidly in the A·U region of the hairpin with a

Author contributions: W.C. and S.D. contributed equally to this work; W.C. and S.D. designed research; W.C. and S.D. performed research; W.C. contributed new reagents/analytic tools; W.C. and S.D. analyzed data; and W.C., I.T., and C.B. wrote the paper.

The authors declare no conflict of interest.

This article is a PNAS Direct Submission. S.C.K. is a guest editor invited by the Editorial Board.

[§]Present address: Systems Biology, Harvard Medical School, 200 Longwood Avenue, WA 536, Boston, MA 02115.

[§§]To whom correspondence should be addressed. E-mail: carlos@alice.berkeley.edu.

This article contains supporting information online at www.pnas.org/cgi/content/full/0702315104/DC1.

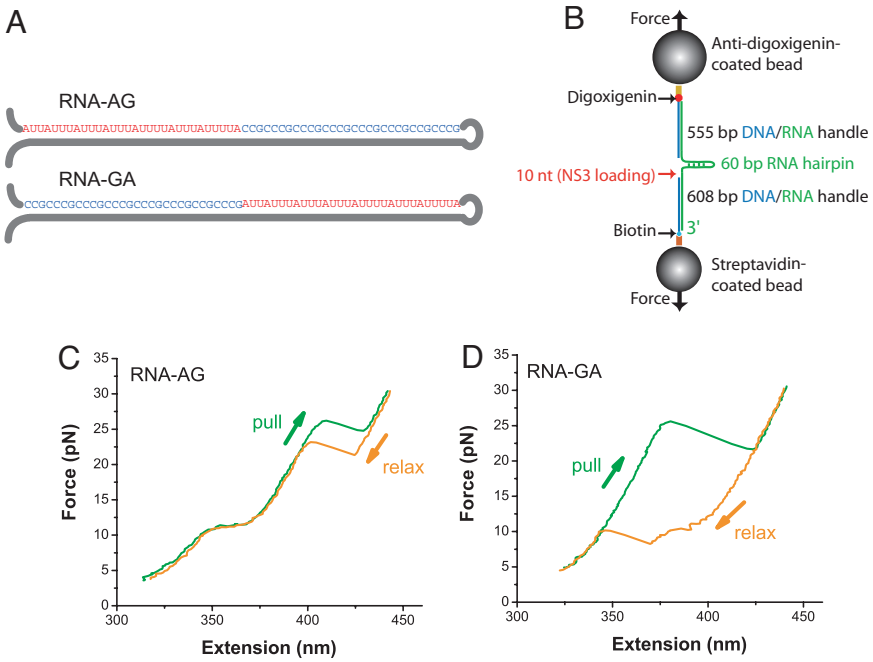


**Fig. 1.** Design and characterization of RNA hairpin substrates for NS3 helicase activity. (*A*) Sequences of substrates RNA-AG and RNA-GA, both containing 60 bp and terminating with a tetraloop. (*B*) Schematic of experimental design using optical tweezers. The ends of a single RNA molecule are attached to two microspheres inside a fluid chamber, one of which is held in an optical trap while the other is held on a micropipette by suction. Spatial and temporal resolutions of 2 nm and 20 ms, respectively, can be achieved with this experimental design. (*C*) Force–extension curves of RNA-AG unfolding (green) and refolding (orange) by mechanical force. (*D*) Force–extension curves of RNA-GA unfolding (green) and refolding (orange) by mechanical force. The mechanical pulling and relaxation speeds are 200 nm/s for both.

mean step size of 11 ± 2 bp and then undergoes a long pause at the boundary (±2 bp) between A·U and G·C regions. Subsequent unwinding of the G·C region by NS3 has a mean step size of 9 ± 2 bp but is characterized by a slow stepping velocity (defined by the slope of the step; see *Materials and Methods*) and long pauses. Most unwinding trajectories were followed by a sharp decrease in the extension of the molecule due to dissociation of the helicase and rezipping of the hairpin. In contrast, when G·C pairs are placed in front of A·U pairs (RNA-GA), unwinding events are >50-fold less frequent than RNA-AG when the molecule is held at 7 pN. Frequent unwinding is observed when the molecule is under higher tension to help the enzyme enter and unwind the G·C region. As shown in Fig. 2*B* at 17 pN, the slow unwinding of the G·C region is followed by a sharp increase in the extension of the RNA to a fully unfolded state, because under these forces the A·U region of RNA-GA is already mechanically unstable.

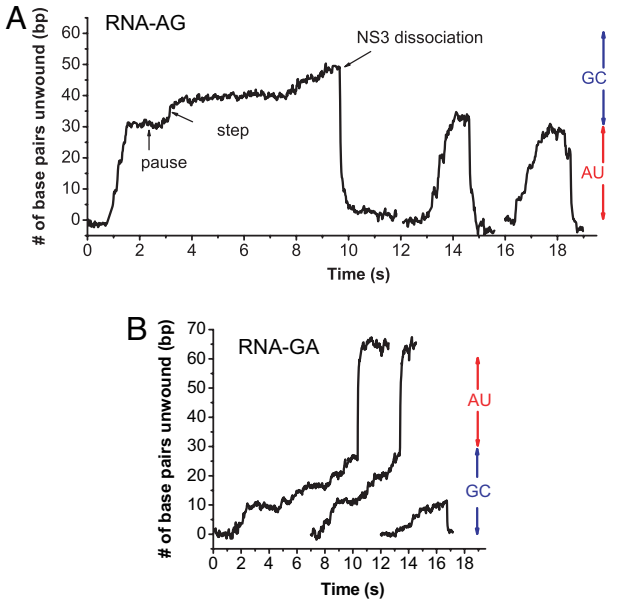


**Fig. 2.** Sequence barriers in an RNA hairpin affect NS3 unwinding kinetics. Representative extension versus time unwinding traces from independent experiments at 7 pN force for RNA-AG (*A*) and at 17 pN force for RNA-GA (*B*). The traces are arbitrarily shifted along the time axis for clarity of display.

Clearly, the pause duration and the stepping velocity of NS3 are both affected by the barriers in RNA, regardless of their location in the hairpin. More importantly, the fact that NS3 undergoes a long pause even before stepping into the G·C region (see arrows in Fig. 2*A*) indicates that the enzyme pauses in front of still intact, stable base pairs. Barrier effects on the dynamics of NS3 are quantitatively summarized in Table 1. Briefly, the mean pause duration in front of the G·C segment is 10-fold longer than that before the A·U segment, whereas the corresponding mean stepping velocity is 3-fold slower. Previous results indicate that force affects neither pause duration nor stepping velocity, which is also confirmed in this study for RNA-AG unwinding (SI Table 2). We have shown previously that the pause is part of the helicase enzymatic cycle and that exit from the pause is not due to binding of multiple helicase molecules (4). The fact that barriers affect pause duration more than stepping velocity indicates that pausing and stepping are associated with different biochemical events during NS3 unwinding. Previously, single-molecule unfolding experiments have been used to determine the strength and location of the various mechanical barriers in RNA (11). The above results show that these barriers indeed affect the activity of NS3 *in vitro* and therefore are likely to be relevant to the *in vivo* functionality of RNA-based motors.

**Table 1. Dependence of NS3 unwinding kinetics on duplex RNA sequence**

| Sequence | Pause duration, s | Stepping velocity, bp/s |
|---|---|---|
| 100% A·U | 0.20 ± 0.03 | 62 ± 26 |
| 52% G·C | 0.60 ± 0.06 | 51 ± 26 |
| 100% G·C | 2.0 ± 0.3 | 22 ± 17 |

Data from RNA-AG were analyzed for pause duration and stepping velocity on 100% A·U and 100% G·C; data from RNA3 (4) were analyzed for pause duration and stepping velocity on 52% G·C. The RNA3 substrate was characterized previously and has the following sequence: GGGAGCACUACGUUCGGACUAGUGUACUCUGACUUGAGACUACUGACAUCCAGAUCUCCCCCATGGGAGAUCUGGAUGUCAGUAGUCUCAAGUCAGAGUACACUAGUCCGAACGUAGUGCUCCC, where the 4-nt tetraloop is underlined. Numbers of traces included in the analysis were 96 and 102 for RNA-AG and RNA3, respectively. For RNA-AG, traces were at 7 pN; for RNA3, traces were at 17 pN.

**Analysis of Stepping Velocity Indicates Active Unwinding.** While steps coincide with base pair opening by NS3, the barrier-dependent pause durations suggest that during a pause, NS3 either passively awaits the spontaneous fraying of the duplex to move or actively interacts with the duplex for a duration that depends on the stability of the latter. Analysis of the stepping velocity at various barriers furnishes a way to establish this point. In the first case, unwinding is a passive process; the enzyme establishes no destabilizing interactions with the RNA and only moves forward opportunistically, upon spontaneous thermal fraying of the duplex (5, 7). Because the kinetics of thermal fraying is much faster than that of helicase movement (17, 18), the opening and closing of RNA base pairs can be assumed to be in rapid equilibrium when compared with the rate constant of helicase forward movement (see *SI Text*). In these circumstances, it is the free energy of base pair opening rather than the activation energy that determines how fast the helicase unwinds. As we derive (see *SI Text*), the mean stepping velocity of a passive helicase can be written as a function of the rate of helicase translocation (19, 20) on ssRNA and the thermodynamic stability of base pairs in front of the helicase (see *SI Text*):

$$\ln v = \ln s + \ln k_3 - \ln\left[1 + c\,\exp\left(\frac{\Delta G^\circ_{\text{open}}}{RT}\right)\right], \qquad [1]$$

where $v$ is the mean stepping velocity, $s$ is the step size of the helicase, $k_3$ is the rate constant of helicase translocation on ssRNA and is assumed to be sequence-independent, and $c$ gives the contribution of external force to base pair free energy, $c = \exp[-F\Delta x/(k_B T)]$, where $F$ is the force on the substrate and $\Delta x$ is the end-to-end extension change in the substrate upon opening of $s$ base pairs at force $F$. Importantly, by definition, a passive helicase does not change the energetics of base pairs and, thus, $\Delta G^\circ_{\text{open}}$ is simply the standard free energy to open $s$ base pairs at zero force and can be estimated from nearest-neighbor stability data (21).

To determine the extent to which NS3 relies on thermal fraying, we plotted the stepping velocity expected from this model for a purely passive helicase as a function of $\Delta G^\circ_{\text{open}}$ (Fig. 3*A* and SI Fig. 8) and compared it with the stepping velocity of NS3. As shown by the dashed line in Fig. 3*A*, the stepping velocity of a purely passive helicase decreases with increasing free energy of base pair opening. Interestingly, the stepping velocity of NS3 (blue symbols) is less sensitive to the presence of barriers than what is expected for a passive helicase. In particular, for the opening of 4 bp, equivalent to one substep of NS3 observed previously (4), the mean stepping velocity of NS3 on G·C base pairs is >14,000-fold faster than a passive helicase, indicating that NS3 actively reduces the free energy of base pair opening. We also performed calculations for substeps of other sizes (SI Fig. 8). For a 1-bp substep (22), the stepping rate of NS3 is still 2- to 3-fold faster than a passive helicase on substrates with 50% or more GC content (Fig. 3*B*). Thus, rather than passively awaiting the thermal fraying of the RNA, NS3 interacts with the duplex and actively speeds up RNA unwinding.

To lower the free energy of base pair opening, the helicase can either destabilize the dsRNA or stabilize the separated single strands upon unwinding. To distinguish between these two possibilities, we investigated how the durations of the pauses preceding the NS3 steps depend on the barrier ahead. We found that pause durations are much shorter than those expected for a passive helicase (Fig. 3*C*), a result consistent again with a scenario in which NS3 does not passively wait for the thermal fraying of base pairs before stepping but instead actively destabilizes the RNA duplex during the pause. This conclusion is also supported by calculations done for 1-, 2-, 3-, and 5-bp openings (data not shown). The minimum amounts of free energy reduction in base pair opening introduced by the active enzyme, calculated from Fig. 3*A*, are 1.8, 6.7, and 10.1 *RT* for 4 bp made up of 100% A·U, 52% G·C, and 100% G·C, respectively (*SI Text* and SI Table 3).

**Barrier Dependence of NS3 Processivity and Residence Time.** Next, to understand the interaction of NS3 with the RNA substrate, we investigated how the barriers present in RNA influence the

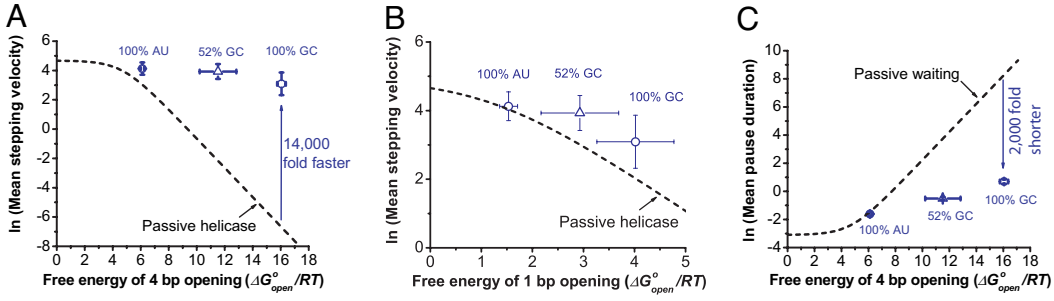


**Fig. 3.** NS3 moves on RNA by destabilizing duplex RNA. (*A*) The mean stepping velocity of NS3 (blue symbols) depends much less on $\Delta G^\circ_{\text{open}}$ than a passive helicase (dashed line), where the stepping velocity for 52% G·C was taken from a previous study (4). The free energy is in units of *RT*, where *R* is the gas constant and $T = 295$ K. The *y*-intercept of the dashed line is set identical to the *y*-intercept of a straight line that fits NS3 stepping velocity. This straight line (not shown) gives a slope of −0.09 for 4 bp being unwound each time and defines an upper bound of 106 $s^{-1}$ for NS3 stepping velocity on dsRNA. (*B*) Dependence of helicase mean stepping velocity on the free energy of base pair opening. The dashed line is calculated for a passive helicase with a substep size of 1 bp. (*C*) Dependence of helicase mean pause duration on the free energy of base pair opening. The dashed line is calculated based on Eq. 5 (*SI Text*) at 7 pN for a purely passive helicase. The *y*-intercept given by a straight line (not shown) that fits NS3 data defines a lower bound of 0.02 s for NS3 pause duration on dsRNA. The *y*-intercept for the dashed line is chosen to be the same as that of the straight line for this comparison. All of the error bars represent 68% confidence interval.

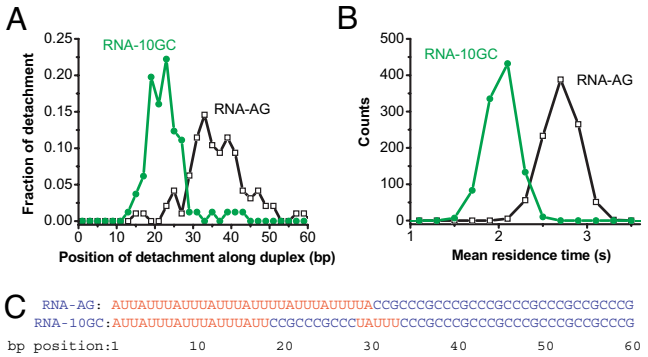


**Fig. 4.** Effects of RNA sequence barriers on NS3 processivity and residence time. (*A*) Detachment of NS3 from the substrate depends on the position of the G·C barrier in dsRNA. Histograms of NS3 detachment along the hairpin stem at 7 pN on RNA-AG (96 traces; open squares) and RNA-10GC (81 traces; filled circles), respectively. (*B*) Distribution of NS3 residence time depends on the presence of the G·C barrier in the RNA hairpin. Analysis is with the same data as in *A*. (*C*) Sequence alignment of hairpin substrates RNA-AG and RNA-10GC. The number below indicates the base pair position along the hairpin stem.

detachment of a single NS3 helicase during unwinding. Fig. 4*A* (open squares) shows a histogram of the fraction of NS3 molecules detached during unwinding of RNA-AG (96 unwinding events). The position at which NS3 dissociates from the substrate can be directly determined from the single-molecule unwinding traces, as indicated by the sharp decrease in the extension of the substrate (Fig. 2*A*). As shown in Fig. 4*A*, the fraction of NS3 detachment is greatest at the boundary between the pure A·U and G·C regions. To determine whether this detachment occurs in response to the G·C barrier and not for other fortuitous reasons, we designed one more substrate, RNA-10GC that has 10 G·C pairs starting at position 19 (Fig. 4*C*). Significantly, we found that the peak position of NS3 detachment changes with the position of the G·C barrier in RNA (Fig. 4*A*, filled circles), a result indicating that the stability of the NS3–RNA complex is affected by the G·C barriers encountered by the enzyme. This experiment also shows that a barrier consisting of 10 G·C pairs is strong enough to trigger significant detachment of the helicase from RNA. A similar effect of barriers on NS3 processivity is revealed by comparing NS3 unwinding on substrates RNA-AG, RNA3, and RNA-GA (SI Fig. 9). From these results, the processivity of NS3 on A·U is estimated to be 150 bp at 9 pN, whereas it is only 12 bp on G·C at 11 pN (see *SI Text*).

Why does NS3 fall off the substrate more frequently upon encountering a barrier? Because a strong barrier induces the helicase to pause, a possible answer is that NS3 may have a higher probability of detachment while pausing than while stepping. However, analysis of all processivity data indicates that NS3 is no more likely to detach from the substrate when pausing than when translocating along the RNA. Alternatively, a simple model of competition between on-pathway unwinding and off-pathway detachment can explain these observations (23). Strong barriers lengthen the duration of NS3 pauses, therefore increasing the chance of the enzyme to move off of the main helicase pathway and dissociate. This conclusion would be valid for either a passive or an active helicase. In particular, for a passive helicase that contacts the ssRNA region and waits opportunistically for the fraying of the duplex without actively interacting with it, the mean residence time (i.e., the average time that the helicase stays on the substrate before detachment) should be the inverse of the helicase off-rate on ssRNA and independent of the position and magnitude of the barriers in the substrate (24). This is, however, not the case for NS3; rather, the residence time of NS3 on RNA depends on the presence of a barrier as shown in Fig. 4*B*. RNA-10GC contains a strong G·C barrier from base pair 19 to 28, whereas RNA-AG contains all A·U pairs in this region. The mean residence time of NS3 on RNA-AG is 2.70 ± 0.02 s as compared with 2.00 ± 0.02 s on RNA-10GC. The effect of strong barriers on the residence time of NS3 on RNA suggests an active interaction between NS3 and the barrier, which for stronger barriers leads to the accelerated detachment of the helicase (24). Indeed, the rate coefficient of NS3 dissociation upon unwinding G·C sequences is 0.5 ± 0.2 $s^{-1}$ at 7 pN, which is 2-fold faster than that on A·U sequences at the same force. These results are inconsistent with a purely passive helicase (24) but reveal a motor that actively destabilizes and separates the RNA strands. The picture that emerges then is one in which the enzyme must interact with the dsRNA to destabilize the duplex, and failure to do so speeds up the enzyme detachment from the substrate.

**Tunable Response of NS3 to Sequence Barriers.** The model described above predicts that the probability of enzyme dissociation should depend on the physical size of the barrier (i.e., the number of G·C pairs), because its size will determine the stability of the barrier and the tendency of the duplex to rezip. To test this model, we designed two more RNA hairpin substrates (Fig. 5*A*). Instead of having all A·U pairs followed by G·C pairs, substrate RNA-6GC has 22 A·U pairs followed first by 6 G·C pairs, then 5 A·U pairs, and then 27 G·C pairs; while substrate RNA-3GC has 22 A·U pairs followed first by 3 G·C pairs, then 5 A·U pairs, and then 30 G·C pairs. We first characterized the mechanical unfolding properties of these substrates. As shown in SI Fig. 10*A*, RNA-6GC unfolds in three transitions by mechanical force; the unfolding of the first 22 A·U pairs occurs at 11.5 ± 0.1 pN; the next 6 G·C pairs followed by 5 A·U pairs unfold at 20.5 ± 0.2 pN; and the next 27 G·C pairs unfold at 25.8 ± 0.3 pN. RNA-3GC also unfolds in three transitions by mechanical force (SI Fig. 10*B*), but the second transition corresponding to 3 G·C pairs and 5 A·U pairs occurs at 17.0 ± 0.1 pN.

The unwinding of RNA-6GC and -3GC by NS3 is shown in Fig. 5 *B* and *C*, respectively. Most unwinding events on RNA-6GC show the effect of the 6 G·C pairs spanning positions 23–28 with NS3 responding either by detachment or a long pause followed by rapid unwinding upon encountering the barrier. In contrast, most unwinding events on RNA-3GC do not show any significant effect of the first 3 G·C pairs on NS3 unwinding and processivity but undergo long pauses or detachment when NS3 faces the second G·C barrier in the substrate. These observations are quantitatively summarized in Fig. 5*D* by using a cumulative processivity plot, which describes the fraction of unwinding events at each duplex length taking place before detachment. The preferential detachment of NS3 on RNA-6GC over -3GC shows that NS3 processivity depends on the strength of the barrier. Most interestingly, although RNA-6GC and -3GC are identical in sequence up to base pair 25 (indicated by the dashed line in Fig. 5*D*), the fraction of NS3 molecules that dissociate begins to differ at base pair 20 and at base pair 25 already differs by 40% between these two substrates. These results reveal that the probability of NS3 detachment depends on the sequence ahead of the opening fork as far as 6 bp. RNA thermodynamic stability is well described by nearest-neighbor interactions (21). The fact that NS3 detachment is affected by RNA 6 bp away from the opening fork indicates that NS3 interacts with the duplex RNA at least 6 bp ahead of the fork and that this interaction, in turn, affects the stability of the enzyme–substrate complex.

## Discussion

To rationalize the above observations, we propose a model for the movement of NS3 as it unwinds an RNA duplex. In this model, NS3 makes at least two points of contact with the substrate; one at the fork, possibly tracking the ssRNA during

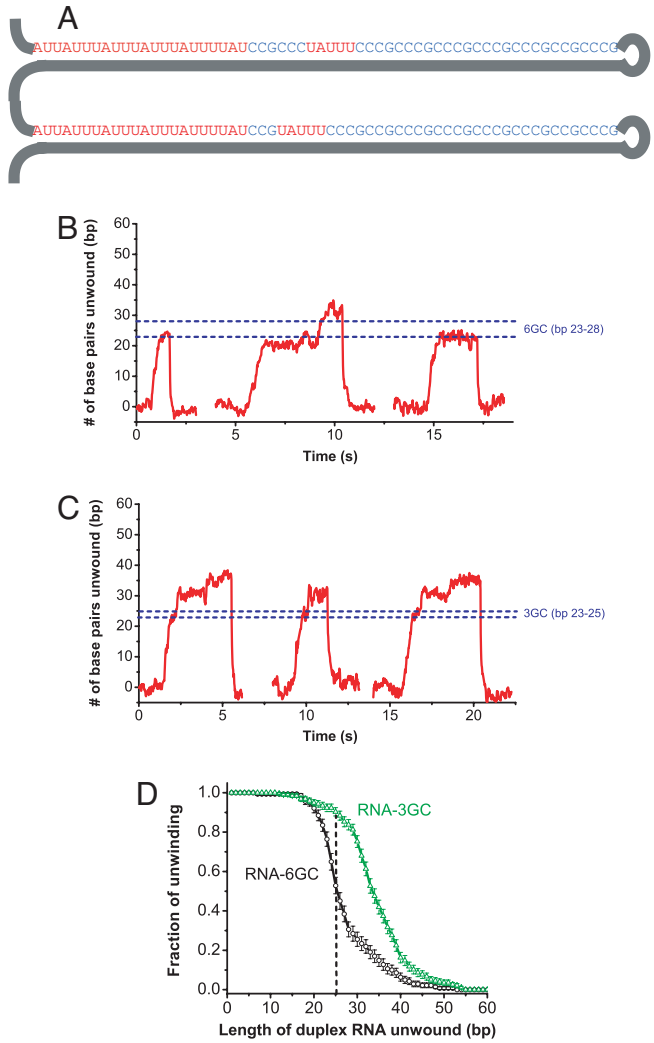


**Fig. 5.** NS3 senses barriers ahead of the opening fork with a tunable response. (*A*) Sequences of substrates RNA-6GC and RNA-3GC, both containing 60 bp and terminating with a tetraloop. (*B* and *C*) Representative extension vs. time unwinding traces from independent experiments at 7 pN for RNA-6GC and RNA-3GC, respectively. The traces are arbitrarily shifted along the time axis for clarity of display. (*D*) Cumulative processivity plots comparing the processivity of NS3 on RNA-6GC (black) and RNA-3GC (green). RNA-6GC and -3GC are identical in sequence up to base pair 25 (dashed line). The data were constructed from unwinding traces at 7 pN constant force for RNA-6GC (140 traces) and RNA-3GC (196 traces), respectively.

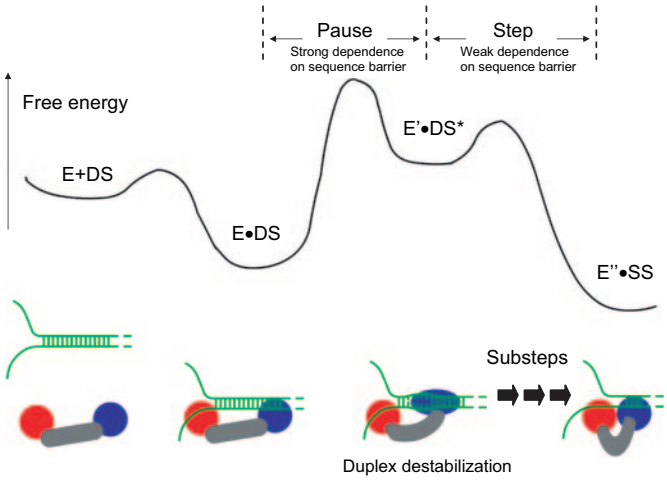


**Fig. 6.** Model for NS3 helicase interaction with the substrate RNA during active unwinding. The helicase (E) binds to dsRNA (DS) to form the complex E·DS. After this complex formation, the helicase destabilizes the duplex ahead of the opening fork. Depending on the strength of the barrier ahead, success in destabilization leads to the formation of helicase–substrate complex E′·DS*. In single-molecule experiments, this transition from E·DS to E′·DS* corresponds to pause of NS3 in front of a barrier. During the pause, strand separation has not yet occurred at the fork. Failure of the helicase to cross the barrier between E·DS and E′·DS* leads to detachment from RNA. The complex E′·DS* can proceed to form the NS3–product complex (E″·SS), which occurs through NS3 substeps (4). This strand-separation process is less dependent on barriers than the pause. After substeps, the helicase resets to E·DS and starts the next cycle of pausing and stepping. The various states of the helicase and the substrate RNA are schematically depicted in the cartoons below the free energy diagram.

active unwinding, and the other ahead of the fork, contacting the duplex RNA to (*i*) actively destabilize it during the pause preceding the step and (*ii*) establish new thermodynamically more favorable interactions with the RNA (see Fig. 6 for a free energy diagram and a cartoon model of these interactions). The processivity of the enzyme depends on the formation of a stable contact with the RNA ahead. Such a contact may involve partial melting of the duplex and, therefore, its duration should be barrier-dependent. It is easier for the enzyme to form a stable contact on A·U than on G·C sequences because A·U duplexes are thermodynamically less stable. Depending on the strength of the barrier (affected variously by its sequence, its length, etc.), the interaction with duplex RNA ahead of the fork leads to either stabilization of the NS3–RNA complex competent for unwinding or the accelerated detachment of NS3 from the substrate. We term this phenomenon "barrier sensing." In the latter case, NS3 dissociates from the RNA even before the duplex is unwound. A very important prediction of this model is that once NS3 succeeds in making a stable contact with the RNA ahead, the speed of subsequent strand separation as defined by the stepping velocity should be less sensitive to the strength of the barriers, because the free energy of base pair opening has already been lowered by the helicase at the end of a pause. Indeed, the stepping velocity of NS3 on A·U versus G·C only differs by 3-fold, in contrast to the 10-fold difference in the mean pause duration before stepping (Table 1), and NS3 stepping velocity is much faster than that of a passive helicase (Fig. 3*A*). The "two points of contact" model presented here is consistent with the inchworming mechanism previously proposed for this enzyme (4) and also with the sensitivity of NS3 helicase activity to the structure of the duplex from bulk studies (25).

Collectively, our data strongly favor NS3 being an active helicase instead of a purely passive Brownian ratchet. Lohman and coworkers (26, 27) have conducted elegant pre-steady-state bulk experiments to test whether a helicase uses a passive or an active mechanism of unwinding. In these experiments, it was shown that Rep or UvrD helicase can bypass a non-DNA linker between duplex and single-stranded DNA (ssDNA) tail to unwind duplex DNA *in vitro*. These results argue against a type of passive model in which the unidirectional translocation of the helicase along ssDNA leads to unwinding of the substrate.

Mechanical force has been used to study folding and unfolding of single RNA molecules (11, 13) (SI Fig. 11). However, it remained unclear how relevant the information deduced from these studies is to biochemical processes involving RNA helicases and other motors, such as ribosomes, that must unwind dsRNA regions during their translocation. The present study validates the results of single RNA molecule unfolding experiments by revealing an important correspondence between mechanical force and the enzymatic action of the NS3 helicase: duplex sequences that require a higher mechanical force to

unfold and constitute barriers in mechanical unfolding experiments also cause the helicase to pause longer and to move slower.

Numerous nucleic acid translocases were shown to move at rates limited by the thermal fraying of nucleic acid base pairs (7, 28). In contrast to these enzymes, NS3 moves on nucleic acids faster than the rate imposed by the thermal fraying of base pairs. We propose that this faster, catalyzed movement is facilitated by a decrease of the stability of the RNA duplex brought about by contacts between the helicase and duplex RNA ahead of the opening fork. The sensitivity of NS3 helicase to sequence barriers in RNA should be relevant to a broad range of motors using RNA as substrate, such as ribosomes that translate through secondary structures in mRNAs (29) and whose dynamics (pauses, rate of translocation, and frame-shifting) may depend on the sequence barriers encountered therein.

## Materials and Methods

**RNA Substrates and NS3 Protein.** The RNA molecules used throughout this study were all made from *in vitro* transcription using T7 RNA polymerase (Ambion) as described (4) with modifications. The detailed procedures are reported in *SI Text*. Full-length NS3 from HCV genotype 1a was overexpressed in M15(pRep4) (Qiagen) and purified by using the protocol described in ref. 30. NS3 concentration was measured by using absorbance at 280 nm ($\varepsilon = 6.36 \times 10^4$ $M^{-1}{\cdot}cm^{-1}$ in 20 mM sodium phosphate buffer with 6 M guanidinium chloride, pH 6.5). Bulk unwinding assays under single-turnover conditions indicated that the NS3 monomer does have helicase activity at zero force (SI Fig. 7).

**Optical Tweezers Experiments.** We used a counterpropagating dual-beam optical tweezers instrument (12) to manipulate individual RNA molecules. Unless otherwise noted, the force–extension measurements of the RNA hairpin were done at 22 ± 1°C in standard buffer (10 mM Tris·Cl/100 mM NaCl, pH 7.0), and the helicase unwinding experiments were done as described (*SI Text*) at 22 ± 1°C in buffer U (20 mM MOPS/30 mM NaCl/0.9% vol/vol glycerol/0.75 mM $MgCl_2$/0.1% Tween 20/2 mM DTT, pH 6.5).

**Data Analysis.** NS3 steps and pauses were analyzed as described previously by using a custom-written MATLAB program (4). To examine whether a detachment of the helicase is within a step or within a pause, the shortest pause was required to be longer than 70 ms. To calculate the distribution of NS3 mean residence time on a substrate, a random sampling analysis of NS3 residence time was performed. For unwinding traces collected for a given RNA substrate, 50 traces were randomly chosen each time to compute the mean residence time. This random selection process was repeated 1,000 times to obtain the distribution of the resulting mean residence time. The errors for step size and stepping velocity were standard deviations. The errors for pause duration and residence time were standard errors of the mean. The errors for fraction of unwinding were standard deviations obtained from bootstrap analysis for the same data sets sampled 1,000 times.

We thank Anna Marie Pyle (Yale University, New Haven, CT) and Rudolf K. Beran (Yale University) for generously providing NS3 proteins to start this project and for helpful comments on this work; Prof. Charles Rice (Rockefeller University, New York, NY) for kindly providing NS3 plasmid; Steve Smith and Pan Li for technical help and discussions; and Jeff Vieregg, Jeff Moffitt, Eric Galburt, Maumita Mandal, and other members of the Bustamante laboratory for critical reading of the manuscript. This work was supported by the Canadian Institutes of Health Research (S.D.), the National Institutes of Health (I.T. and C.B.), and the Department of Energy (I.T. and C.B.).

1. Rocak S, Linder P (2004) *Nat Rev Mol Cell Biol* 5:232–241.
2. Jankowsky E, Gross CH, Shuman S, Pyle AM (2000) *Nature* 403:447–451.
3. Serebrov V, Pyle AM (2004) *Nature* 430:476–480.
4. Dumont S, Cheng W, Serebrov V, Beran RK, Tinoco I, Jr, Pyle AM, Bustamante C (2006) *Nature* 439:105–108.
5. Betterton MD, Julicher F (2005) *Phys Rev E* 71:011904.
6. Lohman TM, Bjornson KP (1996) *Annu Rev Biochem* 65:169–214.
7. von Hippel PH, Delagoutte E (2001) *Cell* 104:177–190.
8. Levin MK, Gurjar M, Patel SS (2005) *Nat Struct Mol Biol* 12:429–435.
9. Gorbalenya AE, Koonin EV (1993) *Curr Opin Struct Biol* 3:419–429.
10. Tan SL, Pause A, Shi Y, Sonenberg N (2002) *Nat Rev Drug Discovery* 1:867–881.
11. Onoa B, Dumont S, Liphardt J, Smith SB, Tinoco I, Jr, Bustamante C (2003) *Science* 299:1892–1895.
12. Smith SB, Cui Y, Bustamante C (2003) *Methods Enzymol* 361:134–162.
13. Liphardt J, Onoa B, Smith SB, Tinoco IJ, Bustamante C (2001) *Science* 292:733–737.
14. Woodside MT, Behnke-Parks WM, Larizadeh K, Travers K, Herschlag D, Block SM (2006) *Proc Natl Acad Sci USA* 103:6190–6195.
15. Smith SB, Finzi L, Bustamante C (1992) *Science* 258:1122–1126.
16. Bustamante C, Marko JF, Siggia ED, Smith S (1994) *Science* 265:1599–1600.
17. Bonnet G, Krichevsky O, Libchaber A (1998) *Proc Natl Acad Sci USA* 95:8602–8606.
18. Snoussi K, Leroy JL (2001) *Biochemistry* 40:8898–8904.
19. Kim DE, Narayan M, Patel SS (2002) *J Mol Biol* 321:807–819.
20. Fischer CJ, Maluf NK, Lohman TM (2004) *J Mol Biol* 344:1287–1309.
21. Turner DH (2000) in *Nucleic Acids: Structures, Properties, and Functions*, eds Bloomfield VA, Crothers DC, Tinoco I, Jr (University Science Books, Herndon, VA), Chap 8.
22. Tomko EJ, Fischer CJ, Niedziela-Majka A, Lohman TM (2007) *Mol Cell* 26:335–347.
23. Galletto R, Jezewska MJ, Bujalowski W (2004) *J Mol Biol* 343:101–114.
24. Betterton MD, Julicher F (2005) *J Phys Condens Matter* 17:S3851–S3869.
25. Tackett AJ, Wei L, Cameron CE, Raney KD (2001) *Nucleic Acids Res* 29:565–572.
26. Amaratunga M, Lohman TM (1993) *Biochemistry* 32:6815–6820.
27. Lohman TM, Hsieh J, Maluf NK, Cheng W, Lucius AL, Fischer CJ, Brendza KM, Korolev S, Waksman G (2003) *The Enzymes* 23:303–369.
28. van Oijen AM, Blainey PC, Crampton DJ, Richardson CC, Ellenberger T, Xie XS (2003) *Science* 301:1235–1238.
29. Takyar S, Hickerson RP, Noller HF (2005) *Cell* 120:49–58.
30. Beran RK, Bruno MM, Bowers HA, Jankowsky E, Pyle AM (2006) *J Mol Biol* 358:974–982.